https://doi.org/10.26599/JAC.2023.9220809

Research Article

Patterned phosphor-in-glass films with efficient thermal management for high-power laser projection display

Zezhong Yang [a], Song Zheng [a], Guoyu Xi [a], Tao Pang [b], Shaoxiong Wang [a], Qingying Ye [a, *], Bin Zhuang [a], Daqin Chen [a, c, d, *]

[a] College of Physics and Energy, Fujian Normal University, Fujian Provincial Key Laboratory of Quantum Manipulation and New Energy Materials, Fuzhou 350117, China

[b] Huzhou Key Laboratory of Materials for Energy Conversion and Storage, College of Science, Huzhou University, Huzhou 313000, China

[c] Fujian Provincial Collaborative Innovation Center for Advanced High-Field Superconducting Materials and Engineering, Fujian Normal University, Fuzhou 350117, China

[d] Fujian Provincial Engineering Technology Research Center of Solar Energy Conversion and Energy Storage, Fujian Normal University, Fuzhou 350117, China

[*]Correspondence: E-mail: qyye@fjnu.edu.cn (Q. Y. Ye); dqchen@fjnu.edu.cn (D. Q. Chen)

Received: August 2, 2023; Revised: September 5, 2023; Accepted: September 20, 2023

Abstract: Recently, high-performance color converters excitable by blue laser diode (LD) have been sprung up for projection display. However, thermal accumulation effect of color converters is a non-negligible problem under high-power LD irradiation. Herein, we developed a novel opto-functional composite (patterned $CaAlSiN_3$: Eu^{2+} phosphor-in-glass film-$Y_3Al_5O_{12}$: Ce^{3+} phosphor-in-glass film@Al_2O_3 plate with aluminum "heat sink") via a thermal management methodology of combining "phosphor wheel" and "heat sink" for the lighting source of high-power laser projection display. This new composite design makes it effective to transport the generated thermal phonons away to reduce thermal ionization process, and to yield stable and high-quality white light with brightness of 4510 lm @ 43 W, luminous efficacy of 105 lm/W, correlated color temperature of 3541 K, and color rendering index of 80.0. Furthermore, the phosphor-in-glass film-converted laser projection system was also successfully designed, showing more vivid color effect than traditional LED-based projector. This work emphasizes the importance of thermal management upon high power laser irradiation, and hopefully facilitates the development of new LD-driven lighting source for high-power laser projection display.

Keywords: phosphor-in-glass (PiG) film; laser-driven lighting; luminescent materials; heat dissipation; glass ceramics

1 Introduction

As an indispensable part in people's daily life, projection display is pursuing for higher brightness and wider color gamut [1-4]. The new lighting technology of light-emitting diode (LED) and laser diode (LD) has gradually replaced the traditional lighting sources with shortcomings of short service life, long response time, and the degradation of lighting quality with long-term usage, such as halogen lamps, high-pressure sodium lamps and high-pressure mercury lamps [5-7]. Among them, LD was proposed as an ideal choice, because of its ultra-narrow bandwidth and free of "efficiency droop" for high-power projection display [8,9]. Due to unparalleled color gamut, using red, green and blue (RGB) LD as a lighting source seems to be a perfect option [10,11]. Nevertheless, RGB LD-based projection is confronted with problems of the scarcity of green laser light, and severe laser speckle noise from the strong coherent of laser [12]. Therefore, using blue LD to excite color converters, as an alternative strategy, has recently sprung up for projection display.

From the perspective of color converters, the phosphors in silicone (PiS) commonly used in white LED will carbonize under high power density laser excitation and become no longer applicable, because of its poor heat resistance and low thermal conductivity [9, 13,14]. In this context, three kinds of all-inorganic color converters - single crystal [15-17], transparent ceramic [18-22] and phosphor in glass (PiG) [23-32] have replaced the phosphor-organic polymer binders, and become the core material for laser-driven lighting source due to their robustness. By contrast, PiG and phosphor-in-glass film (PiGF) have the advantages of cost-effective fabrication, flexible design and tunable luminescence by mixing multi-phase phosphors. To be noted, the glass is a poor conductor of heat in nature, resulting in the fact that PiG easily gets luminescence saturation at low power density of 0.1~3 W mm^{-2} upon blue laser irradiation. PiGF sintered onto the substrate with high thermal conductivity (TC) has more

higher saturation threshold (6~20 W mm^{-2}), and therefore has received great attention [26, 30, 31, 33].

As known, thermal accumulation is a non-negligible problem under high-power LD irradiation. Even for PiGF-on-plate with high TC, efficient thermal management is essential for transporting the generated thermal phonons away and increasing the service life of constructed high-power lighting source [34, 35]. There are generally two approaches to improve the thermal transportation process: "phosphor wheel" [1, 36] and "heat sink" (HS) [28, 29, 33]. However, the saturation threshold is still too low to meet practical application because the neglection of effective combination of structure design and thermal management for the achievable luminescent performance of the constructed high-power lighting source upon blue laser excitation.

Herein, we proposed a patterned PiGF composite material with excellent thermal management, *i.e.*, co-sintering red-emitting PiGF and yellow-emitting PiGF into integration with pattern and coupled with appropriate metallic HS. In this research, the patterned "phosphor wheel" and HS are combined as effective thermal management method. The microstructure, luminescence performance, patterned structure and thermal management methodology have also been systematically studied. Due to the achieved photometric/chromatic controllability and excellent heat dissipation ability of patterned $CaAlSiN_3$: Eu^{2+} PiGF-$Y_3Al_5O_{12}$: Ce^{3+} PiGF@Al_2O_3 plate (abbreviated as "CASN:Eu PiGF-YAG:Ce PiGF@Al_2O_3") with aluminum HS color converter, the constructed brand-new lighting source shows high-quality white light with luminous flux (LF) of 4510 lm @43 W and color rendering index (CRI) of 80.0. Moreover, a high-performance laser-driven projection display based on patterned CASN:Eu PiGF-YAG:Ce PiGF@Al_2O_3 with aluminum HS was experimentally designed for the first time, which exhibits more details of object colors than LED-based projector and demonstrates a great potential in the high-power projection display.

2. Experimental

2.1 Synthesis

Synthesis of glass powders: The precursor borosilicate glass in a composition of SiO_2-B_2O_3-ZnO-Na_2O-Al_2O_3-CaO-BaO-MgO (in mol%) was subjected to glass-melting at 1350 □ for 2 h in a muffle furnace. Subsequently, the melt was casted into a brass mold and further pulverized into powders.

Synthesis of patterned PiGF: The preparation procedure was schematically illustrated in Figure 1. The starting raw materials of prepared glass powders, commercial phosphor ($Y_3Al_5O_{12}$:Ce^{3+} and $CaAlSiN_3$:Eu^{2+}, Grirem Advanced Materials Co., Ltd) as well as the organic vehicles containing 2 ml of ethyl acetate, 1 ml of pine alcohol, and 2.5 g of ethyl cellulose were homogeneously blended by grinding them in an agate mortar. The obtained paste was patterned screen-printed onto the alumina ceramic sheets (Foshan Xinghongfei Electronic Technology Co., Ltd) with thickness of 2 mm and diameter of 25 mm, and then was dried at 120 °C for 1 h to eliminate the organic vehicles. After co-sintering at 640°C for 30 min, the patterned PiGF@Al_2O_3 was obtained eventually. Finally, the patterned PiGF@Al_2O_3 is coupled with a metallic heat sink via using high thermal conductive silicone grease.

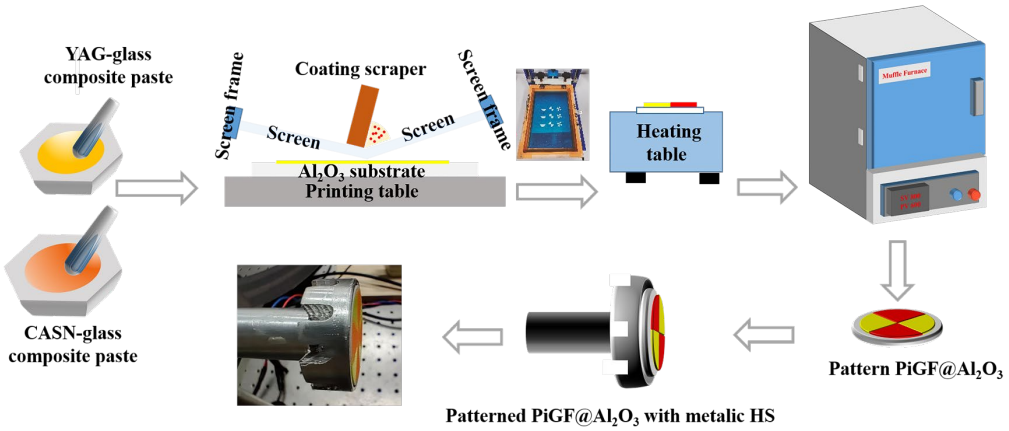

Fig. 1 Fabrication schematic of the patterned PiGF@Al_2O_3 with metallic HS.

2.2 Characterizations

The microstructure observations were conducted by FEI Talos-F200X Transmission Electron Microscope (TEM) operating at 200 kV, and COXEM EM-30 Scanning Electron Microscope (SEM) equipped with an Energy Dispersive Spectrometer (EDS). Confocal inverted microscopy (ECLIPSE Ti2, Nikon, Japan) records the spatial fluorescence distribution in the sample by using a 450 nm xenon light source as the excitation light. X-ray diffraction (XRD) analysis was conducted to determine the phase distribution of PiGFs and associated phosphors using a powder diffractometer (MiniFlex600 RIGAKU) with a Cu Kα radiation source operating at 40 kV in the range of $2\theta = 10°\text{-}70°$ (λ=0.154 nm). Photoluminescence excitation (PLE), PL spectra, fluorescence lifetime and temperature-dependent PL spectra were measured by a fluorescence spectrometer (FLS1000, Edinburgh Instruments, UK). In order to measure the photoluminescence quantum yield (PLQY), the sample was placed in a barium sulfate coated integrating sphere of 15 cm diameter attached to the spectrophotometer. Optical properties of samples under laser excitation, including luminous spectra, luminous flux (LF), luminous efficacy (LE), color correlated temperature (CCT), color rendering index (CRI) and CIE chromaticity coordinates, were measured in a reflection mode using a system consisting of an integrated sphere (30 cm diameter, Labsphere, Inc., USA), a blue laser source (LSR445CP-FC-40 W, Lasever, Ningbo, China) and a CCD spectrometer (HR4000, Ocean Optics, USA) (Figure S1). The irradiated laser spot was tuned by the lens system to a circle with a diameter of 1.8 mm (i.e., corresponding to an area of 2.543 mm^2) (Figure S2). The surface temperature of samples was captured by an infrared thermal imaging camera (TiS75, FLUKE, USA). The infrared thermal imaging camera was placed at 20.0 cm away from the sample and adjusted by its focus.

3. Results and discussion

3.1 Microstructure and luminescence performance

The preparation procedure and home-made laser illumination system were schematically illustrated in Figure 1, Figure S1, S2. The sintering temperature and duration are set as 640 □ for 30 min to fabricate patterned CASN: Eu PiGF-YAG: Ce PiGF@Al_2O_3, based on the overall consideration of the evaporation of organic vehicles and the repair of glass network (Figure S3). The visualization on the cross-section of luminescent patterned CASN: Eu PiGF-YAG: Ce PiGF@Al_2O_3 shows clear boundary between red-emitting CASN: Eu PiGF and yellow-emitting YAG: Ce PiGF by a fluorescent microscope, providing the possibility for the construction of phosphor wheel with patterned structure (Figure 2a). SEM images of YAG:Ce PiGF@Al_2O_3 and CASN:Eu PiGF@Al_2O_3 are shown in Figure 2b, 2c, respectively. YAG:Ce PiGF and CASN:Eu PiGF appear to be densified, which indicates a good wettability of viscous glass flow under the selected preparation condition. The side view of PiGF shows that PiGF is tightly bonded with the Al_2O_3 substrate while the luminescent particles embedded in glass matrix. By repeating the screen-printing process, the film thickness can be well controlled from 40.87 μm to 54.98 μm (Figure S4). The morphology and size of the embedded YAG: Ce particles and CASN:Eu particles have not significantly changed, in comparison with that of the pristine phosphor powders, which indicates that the phosphor does not suffer from serious corrosion by glass composition during the sintering process (Figure 2d, 2e and Figure S5). From the results of accompanied EDS map-scanning analysis, it can be seen that there are obvious rich regions of their own composing elements in the embedded particles, while the signals of borosilicate glass component are very weak in these areas, which confirms their chemical compositions (Figure 2d, 2e).

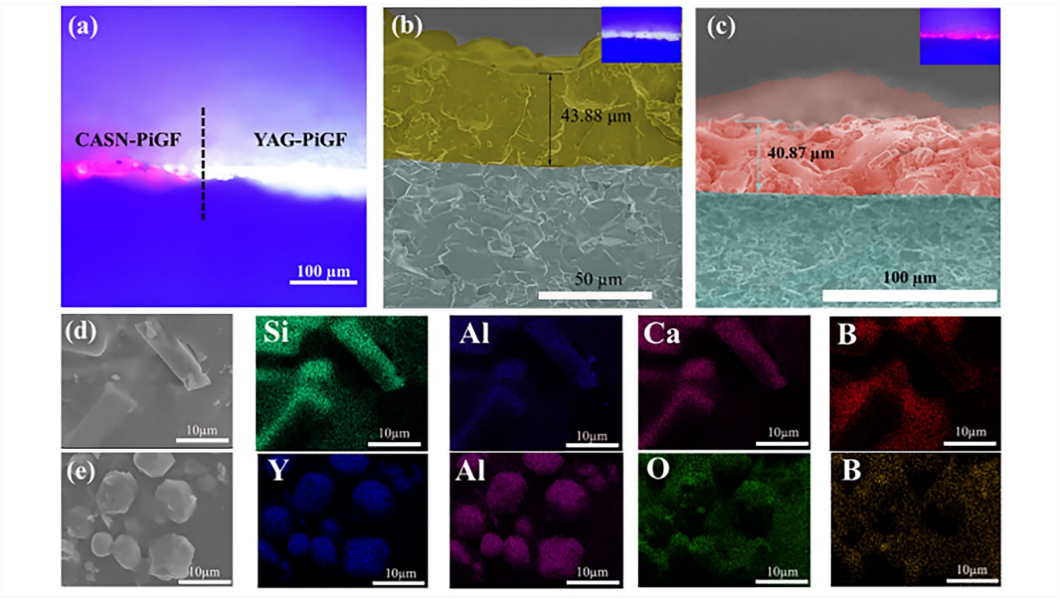

Fig. 2 (a) Visualization on the cross-section of luminescent patterned CASN: Eu PiGF-YAG: Ce PiGF@Al_2O_3 upon 450 nm blue light irradiation. SEM observation on the side view of (b) YAG:Ce PiGF and (c) CASN:Eu PiGF; inset presents the corresponding visualization. SEM image of the enlarged region and accompanied EDS mappings of (d) CASN:Eu PiGF and (e)YAG:Ce PiGF.

In Figure 3a, XRD patterns of YAG:Ce PiGF@Al_2O_3 and CASN:Eu PiGF@Al_2O_3 show that the diffraction peaks are almost identical to their respective phosphor counterparts, except for the amorphous hump from glass matrix and diffraction from alumina plate, with no obvious impurity phases detected. PL and PLE spectra of YAG:Ce PiGF@Al_2O_3 and CASN:Eu PiGF@Al_2O_3 were measured and compared with their phosphor counterparts (Figure 3b). It was found that PL and PLE spectral profiles of samples keep almost invariable after co-sintering, which indicates that the prepared PiGF maintains the luminescent properties of the pristine phosphor. All PL and PLE spectra of them show typical broad emission/excitation bands from Ce^{3+}/Eu^{2+}:5d↔4f parity-allowed transitions [22, 37, 38]. The emission around 690~700 nm is caused by Cr^{3+} emission attributed to 2E→4A transition in the Al_2O_3 substrate [29]. Due to the strong excitation peak at approximately 450 nm, the designed

composite is effectively excitable by blue LD. In fact, the YAG:Ce PiGF@Al_2O_3 and CASN:Eu PiGF@Al_2O_3 samples do yield bright yellow and red emission under blue laser irradiation, respectively, which is consistent with the results above (Figure 3c). In Figure 3d, the corresponding decay lifetimes were evaluated by the equation of $\tau = \int I(t)dt/I_0$, where I_0 is the peak intensity and I(t) is the time-related emissive intensity. The decay lifetimes of YAG:Ce powder, YAG:Ce PiGF, CASN:Eu, CASN:Eu PiGF were all single-exponential fits (χ^2 of 1.06, 0.93, 1.20, 1.26, respectively). The studies on luminescent kinetic decays demonstrate no change in lifetime of YAG:Ce (66.11 ns→63.14 ns) and an obvious lifetime drop of CASN:Eu (670.16 ns→579.84 ns) after co-sintering. Based on the result of CASN: Eu phosphor (lifetime: 580.16 ns) after sintering treatment, it can be deduced that the thermal corrosive effect cannot be trivial for CASN:Eu. However, PLQY of prepared CASN:Eu PiGF@Al_2O_3 can still reach as high as 70.53 % (in comparison, PLQY is 86.27 % for pristine CASN:Eu phosphor) (Figure S6). Meanwhile, PLQY of attained YAG:Ce PiGF@Al_2O_3 is 97.44 %. Compared with YAG:Ce, CASN:Eu is more susceptible to thermal corrosion because of their different chemical composition and thermal stability [26,39]. Given the fact that there is huge heat generated from the irradiation of high-power-density excitation light, the resistance to thermal quenching is very important for color converters. In Figure 3e, 3f and Figure S7, the studies on the temperature-dependent luminescent intensity suggest that due to the encapsulation of robust glass matrix, the resistance to thermal quenching can be obviously improved by transforming phosphor powder form to the glass ceramic film. The PL intensities of YAG:Ce PiGF@Al_2O_3 and CASN:Eu PiGF@Al_2O_3 at ~200 °C can remain 87.06 % and 89.58 % at room temperature, while those of YAG:Ce phosphor and CASN:Eu phosphor are 79.76 % and 83.19 %, respectively.

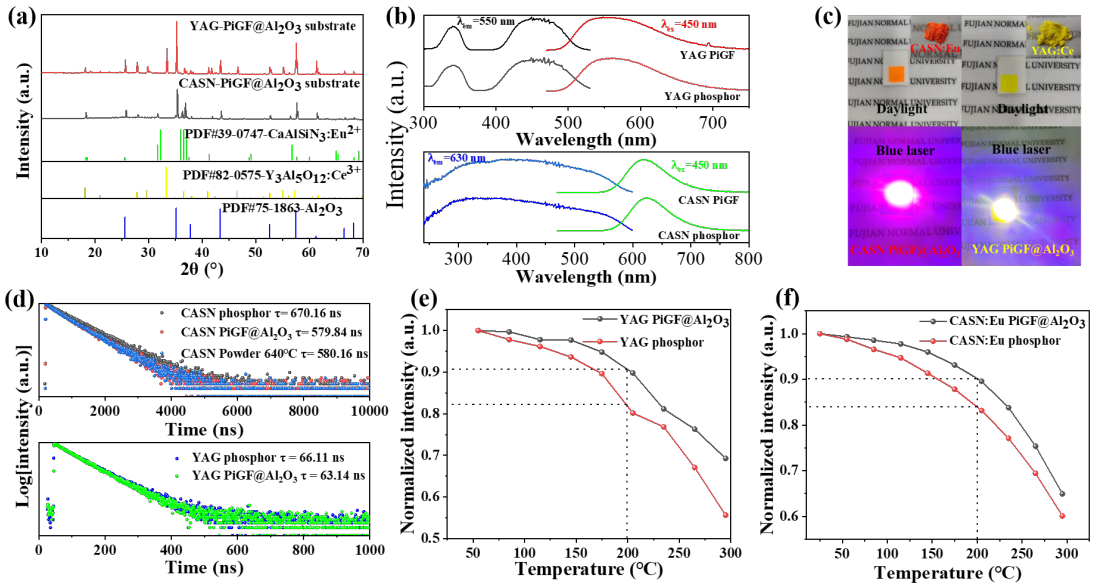

Fig. 3 (a) XRD patterns of YAG:Ce PiGF@Al_2O_3 and CASN:Eu PiGF@Al_2O_3. Comparison made on (b) PL/PLE spectra and (d) luminescent decay curves of YAG:Ce PiGF@Al_2O_3, CASN:Eu PiGF@Al_2O_3 and their phosphor counterparts. (c) Appearance of the YAG:Ce PiGF@Al_2O_3 and CASN:Eu PiGF@Al_2O_3 sample under day light and blue laser light irradiation. (e) Thermal quenching behaviors of YAG:Ce PiGF@Al_2O_3 and YAG: Ce phosphor. (f) Thermal quenching behaviors of CASN:Eu PiGF@Al_2O_3 and CASN:Eu phosphor.

We further attempted to optimize the composite by varying the weight ratio of phosphor powders to glass powders and the film thickness. Through plotting input power density dependent LF, it was found that LF of all YAG:Ce PiGF@Al_2O_3 or CASN:Eu PiGF@ Al_2O_3 samples keeps increasing until gets saturated (Figure S8). Considering that glass is not as a good conductor of heat as Al_2O_3 plate [39], the increase of layer number would reduce the saturation LF and saturation threshold due to the decrease of thermal conductivity (Figure 4a, 4b). Each phosphor could be perceived as a "micro heating source" due to the Stokes shift. A series of experiments were performed by varying the weight ratio of YAG:Ce phosphor powders to glass powders (defined as YtG ratio) and the weight ratio of

CASN:Eu phosphor powders to glass powders (defined as CtG ratio). The saturation threshold also decreases with too much phosphor loaded, because the heat effect will take control the luminescence quenches. The maximal saturation threshold of 12.78 W/mm^2, LF of 5795 lm and LE of 178.3 lm/W is attainable for YAG:Ce PiGF@Al_2O_3 (YtG = 60 %, 1 layer). Meanwhile, the optimized CASN:Eu PiGF@Al_2O_3 (CtG = 30 %, 1 layer) can yield bright red light with LF of 440 lm @ 5.9 W/mm^2.

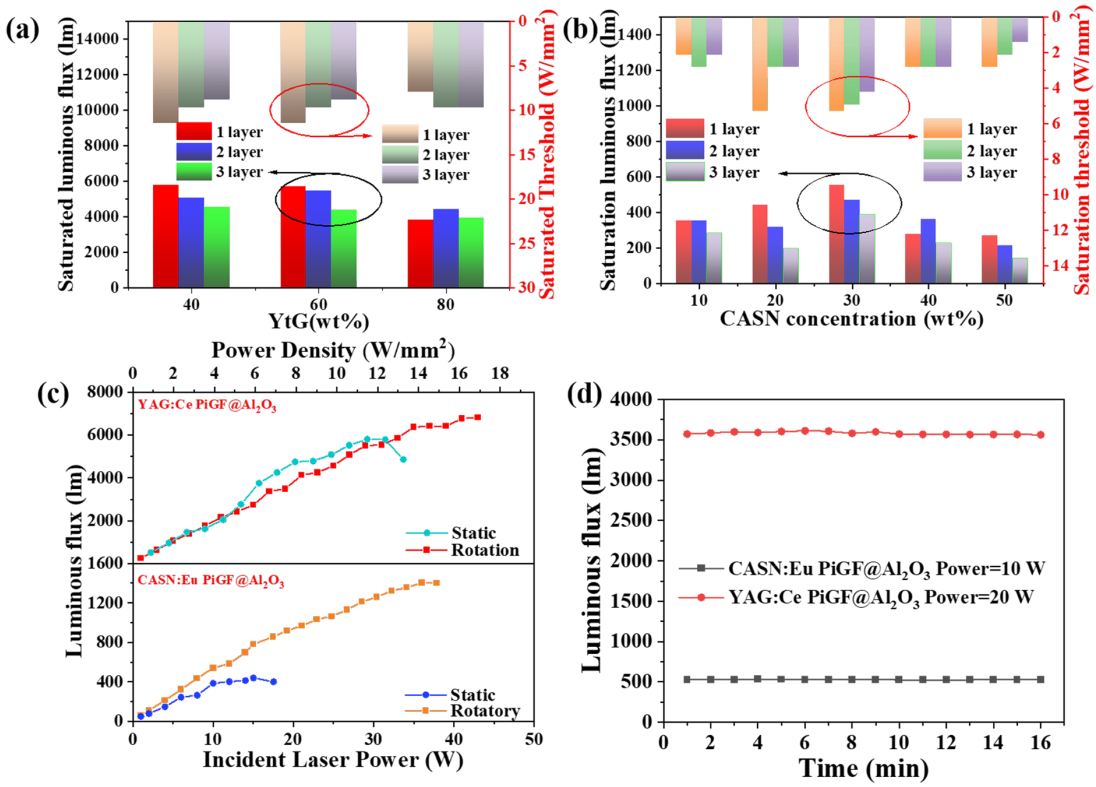

Fig. 4 Saturated LF and saturated threshold of (a) YAG:Ce PiGF@Al_2O_3 and (b) CASN:Eu PiGF@Al_2O_3 with different phosphor contents and different film thicknesses. (c) The derived input power and power density (P_{in}) dependent LF of YAG:Ce PiGF@Al_2O_3 and CASN:Eu PiGF@Al_2O_3 under the various excitation modes (static/rotation). (d) Luminescence intensity variation of the rotated YAG:Ce PiGF@Al_2O_3 and CASN:Eu PiGF@Al_2O_3 "phosphor wheel" upon high-power blue laser irradiation (output optical power: 20 W and 10 W).

The color converters need to cope with the huge heat and high-photon flux irradiation from high-power-density blue LD excitation. The "phosphor wheel" of YAG:Ce PiGF@Al_2O_3 and CASN:Eu PiGF@Al_2O_3 are constructed into a round plate with diameter of 2.5 cm. The "phosphor wheel", on one hand, boosts heat dissipation, and on the other hand, turns the excitation at a point to pulse-like excitation, which leads to the improvement of saturation threshold and luminous brightness. YAG:Ce PiGF@Al_2O_3 and CASN:Eu PiGF@Al_2O_3 show a much higher maximum LF (5795 lm→6827 lm, 440 lm→1402 lm), and exhibit superior saturation threshold of 12.78 W/mm^2 (32.5W)→the power limit 16.9 W/mm^2 (43 W) for blue laser, 5.9 W/mm^2 (15W)→14.2 W/mm^2 (36W) under rotation (Figure 4c), which indicates the effectiveness of "phosphor wheel" [27, 40]. In addition, the stability of lighting sources is also highly concerned. As shown in Figure 4d, when irradiated with high-power blue laser, the luminous intensity of YAG: Ce PiGF@Al_2O_3 and CASN: Eu PiGF@Al_2O_3 can keep stable in the long term.

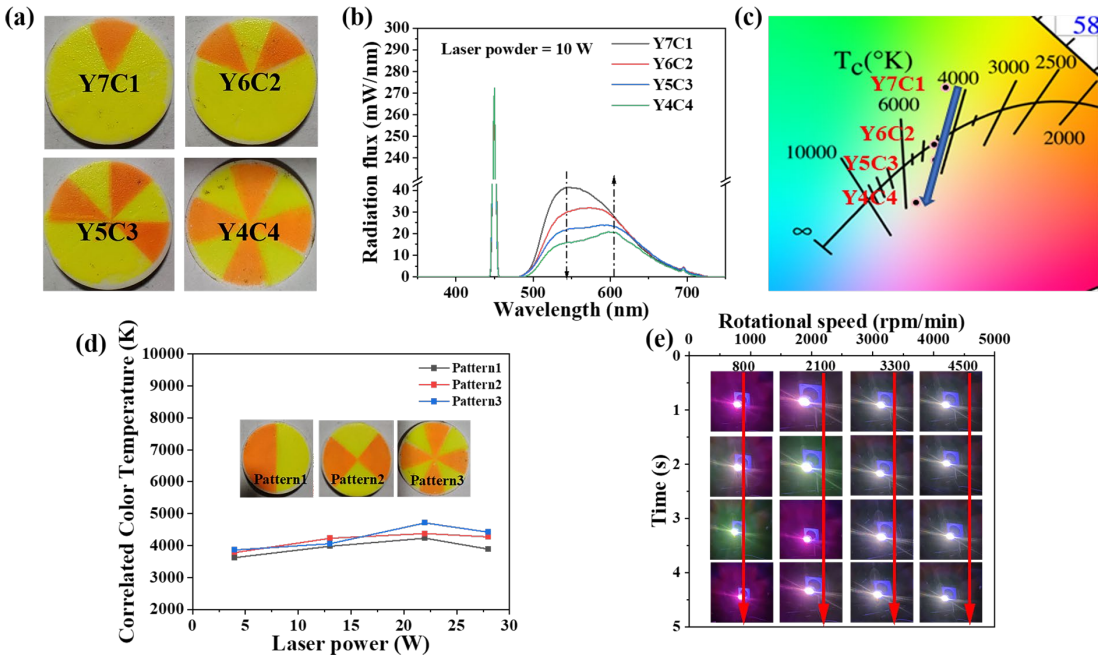

Fig. 5 (a) Photographs of the CASN:Eu PiGF-YAG:Ce PiGF@Al_2O_3 (YtG = 60 %, 1 layer, CtG = 30 %, 1 layer) with different patterned structures. (b) Luminescent spectra and (c) color coordinates of

CASN:Eu PiGF-YAG:Ce PiGF@Al_2O_3 with different patterned structures upon 10 W blue LD excitation. (d) The comparison made on the correlated color temperature (CCT) among the patterned structures with the same total areas between yellow and red. (e) Photographs of the CASN:Eu PiGF-YAG:Ce PiGF@Al_2O_3 phosphor wheel with varying speeds upon 10 W blue-laser driven as time evolves.

The CASN:Eu PiGF-YAG:Ce PiGF@Al_2O_3 samples with different patterned structures were fabricated (Figure 5a). The corresponding luminescence spectra (the input power of 10 W was chosen as a typical case) are presented in Figure 5b. Total areas of yellow and red patterned parts can mediate luminosity and chromaticity. As the area of red patterned part increases, the proportion of red emissive component gradually rises, while the green component decreases. The corresponding color coordinates shifts from yellow-white region to red-white region (Figure 5c and Table 1), due to the variational ratio of the excited blue laser light power to the emission yellow/red light power. Furthermore, if the total areas in red and green parts are the same, there is a very limited difference in photometric/colorimetric parameters among different patterns (Figure 5d). Remarkably, rotation speed exerts important influences on the observed lighting effect (Figure 5e). Only if the rotation speed is over 3300 rpm, the emitting light does look like warm white light because of the human eyes' persistence of vision effect (Movie S1 and Movie S2).

Table 1 Photometric and chromaticity parameters of the CASN:Eu PiGF-YAG:Ce PiGF@Al_2O_3 with different patterned structures upon 10 W blue LD excitation

Patterned structure	CCT (K)	FWHM (nm)	R_a	CIE (x, y)
Y7C1	4548	110.71	57.9	(0.37, 0.43)
Y6C2	4552	121.48	66.1	(0.36, 0.36)
Y5C3	4381	135.88	74.9	(0.36, 0.34)
Y4C4	5088	130.11	80.5	(0.34, 0.29)

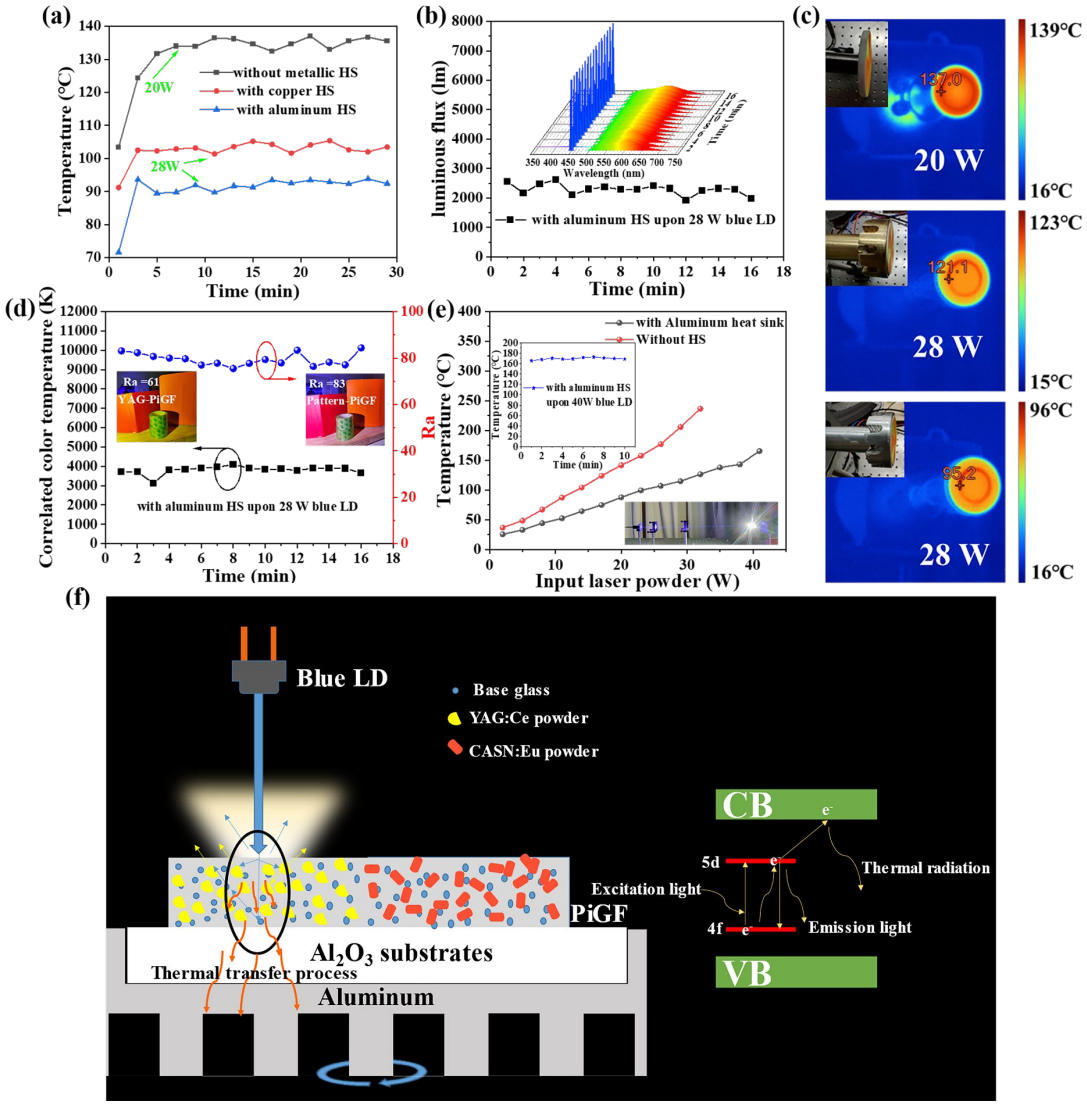

Fig. 6 (a) Local temperature at laser spot for CASN:Eu PiGF-YAG:Ce PiGF@Al_2O_3 with/without metallic HS samples upon blue-laser driven as time evolves. (b) Luminous flux as well as (d) CCT and CRI of CASN:Eu PiGF-YAG:Ce PiGF@Al_2O_3 with aluminum HS upon 28 W blue LD excitation as time evolves; insets of (b, d) shows the corresponding PL spectra and the illumination effect of laser-driven YAG PiGF or patterned PiGF composite white light. (c) The thermal imaging photographs of CASN:Eu PiGF-YAG:Ce PiGF@Al_2O_3 with/without metallic HS samples upon blue-laser driven for 30 min. (e) Local temperature at laser spot of CASN:Eu PiGF-YAG:Ce PiGF@Al_2O_3 with/without metallic HS dependent on incident laser power; insets show the dependence local temperature at laser spot on irradiation duration and the luminescence effect of the developed composite. (f) Schematical

illustration of the enhanced luminescence mechanism by the proposed thermal management methodology.

Solving thermal accumulation effect has recently received great attention for laser-driven lighting sources. The thermal management greatly influences the luminous properties of color converter under blue laser excitation [41, 42]. Aiming at controlling the temperature variation at laser spot as the power increases, the patterned "phosphor wheel" and HS are combined for the first time. When the input blue laser power is increased, the local temperature first increases and then remains unchanged (Figure 6a). The first increase is consistent with the result that the higher input of blue laser leads to the stronger thermal aggregation effect. The subsequent unchanged temperature is caused by the balance between produced heat and exported heat, considering that the rotated phosphor wheel boosts heat convection to air and converts the excitation mode from continuous to pulse-like, and on the other hand, metallic heat sink is a good conductor of heat. The measured time dependent heat dissipation effect for CASN:Eu PiGF-YAG:Ce PiGF@Al_2O_3 with/without metallic HS confirms that heat dissipation is the fastest in the CASN:Eu PiGF-YAG:Ce PiGF@Al_2O_3 with aluminum HS (Figure 6a, Figure S9 and Figure S10). Correspondingly, the maximum surface temperature of CASN:Eu PiGF-YAG:Ce PiGF@Al_2O_3 with aluminum HS is merely ≈95.2 °C @ 28 W under blue LD continuous irradiation for 30 min; and in contrast, those of samples without HS and with copper HS are 137.0 °C @ 20 W and 121.1°C @ 28 W, respectively (Figure 6c). Meanwhile, almost no shift of LF (~2500 lm), CCT (~4000 K) and Ra (~80) occurs for CASN:Eu PiGF-YAG:Ce PiGF@Al_2O_3 with aluminum HS upon 28 W blue LD excitation as time evolves, which complies with the requirements for laser-driven lightings sources (Figure 6b and Figure 6d). These results indicate that the thermal management can well suppress the thermal saturation and improve the luminescence stability of the design composite.

As expected, a very fast temperature elevation up to ~ 236.4 °C and structure destruction was observed in CASN:Eu PiGF-YAG:Ce PiGF@Al_2O_3 without HS within power range of 2 W to 32 W (Figure S11). However, there is only gentle temperature variation (~165.4 °C) in the CASN:Eu PiGF-YAG:Ce PiGF@Al_2O_3 with aluminum HS over a larger power span of 2~43 W (Figure 6e). To be noted, when continually irradiated at 43 W, the surface temperature of CASN:Eu PiGF-YAG:Ce PiGF@Al_2O_3 with aluminum HS remains at approximately 170 °C (inset of Figure 6e). Correspondingly, the emitting white light has CIE color coordinate of (0.378, 0.322), LF of 4510 lm, LE of 105 lm/W, CCT of 3541 K, and CRI of 80.0 (Figure S12). Therefore, it can be found that benefited from the high-thermal-conductivity aluminum HS (~217.7 $W \times m^{-1} \times K^{-1}$) and pulse-like rotatory excitation mode, this novel thermal management method effectively controls the local temperature at the laser spot.

Figure 6f schematically illustrates the mechanism for luminescence enhancement via the proposed thermal management methodology. Each YAG:Ce and CASN:Eu phosphor particle would generate heat because of the Ce^{3+} and Eu^{2+} nonradiative transition upon blue laser irradiation. Due to the combined action of high-thermal-conductivity aluminum HS and rotatory mode, an effective heat conduction network is established to quickly deliver the generated thermal phonons to air, making it difficult for the excited electrons to overcome the energy barrier between Eu^{2+}/Ce^{3+}: 5d level and conduction band minimum (*i.e.*, thermal ionization process), finally enabling efficient luminescence of CASN:Eu PiGF-YAG:Ce PiGF@Al_2O_3 with aluminum HS under high-power blue LD irradiation.

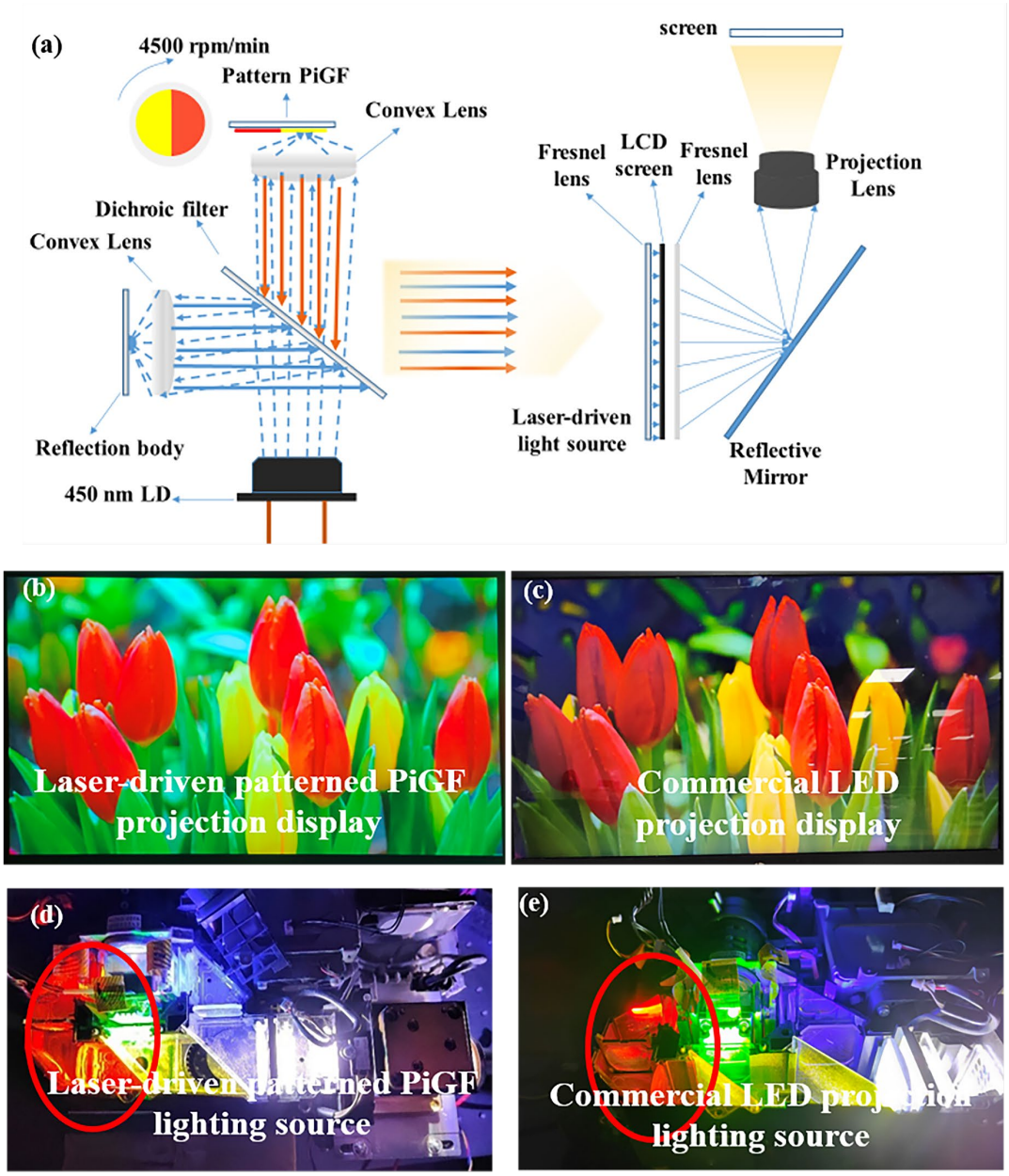

Fig. 7 (a) Illustration of light path for the PiGF-converted laser-driven projection system. (b, c) Projection display performance of PiGF-converted and LED-based projectors, respectively. Sepreating light experiment of (d) developed composite and (e) traditional LED constructed lighting sources for tri-LCD projection display.

In order to evaluate the real effect of the fabricated patterned PiGF composite material with optimized thermal management for high-power laser projection display, we construct a laser-driven

projection system (Figure 7a). The part of blue LD light excites the color converter through the beam splitter, while another part is reflected and combined with the converted light for obtaining lighting source. After further equipping this lighting source in front of the liquid crystal display (LCD) screen followed with a projection lens, a prototype projector is successfully fabricated.

Compared with the traditional LED-based projector refitted based on a commercial projection system (HCP-U32N, Hitachi, Japan), the projection display adopting CASN:Eu PiGF-YAG:Ce PiGF@Al_2O_3 with aluminum HS as color converter exhibits more vivid color with comfortable visual effect (Figure 7b, 7c). For instance, for the projection display of green/red object, the developed projection system presents more intense green/red color and more remarkable color rendition. In addition, the present composite also illustrates the promising application in projector display with tri-LCD, due to the brighter separated light of blue, red and green light from designed composite than traditional LED (Figure 7d, 7e). These results certainly demonstrate the bright prospect of the developed patterned phosphor-in-glass films with efficient thermal management for next-generation high-power laser projection display.

4 Conclusions

In summary, we have proposed an effective thermal management, the combined action of "phosphor wheel" and "heat sink", and developed a patterned $CaAlSiN_3$: Eu^{2+} PiGF-$Y_3Al_5O_{12}$: Ce^{3+} PiGF@Al_2O_3 plate with aluminum HS to high-power laser projection display for the first time. Research suggests that total areas of yellow/red patterned parts and rotation speed have a major impact on the vision effect of emitting light. Under this design, the temperature variation at laser spot is taken control as the power density increases. The optimized patterned $CaAlSiN_3$: Eu^{2+} PiGF-$Y_3Al_5O_{12}$: Ce^{3+} PiGF@Al_2O_3 with aluminum HS can produce stable and high-quality white light with a maximum

luminous flux (LF) of 4510 lm @43 W and color rendering index (CRI) of 80.0. Surprisingly, when continually irradiated at 43 W (the power limit for blue laser), the surface temperature of CASN:Eu PiGF-YAG:Ce PiGF@Al_2O_3 with aluminum HS remains at approximately 170 °C, while a very fast temperature elevation up to ~ 236.4 °C and structure destruction are observed in CASN:Eu PiGF-YAG:Ce PiGF@Al_2O_3 without HS within power range of 2 W to 32 W. Finally, we have constructed laser-driven projection display system to evaluate the application feasibility of developed composite materials. Compared with the traditional LED-based projector, the demo based on CASN:Eu PiGF-YAG:Ce PiGF@Al_2O_3 with aluminum HS as color converter exhibits better display effect. Therefore, this study demonstrates an effective design to develop lighting source of for high-power laser projection display.

Acknowledgements

This research was supported by National Key Research and Development Program of China (2021YFB3500503), National Natural Science Foundation of China (52272141, 51972060, 12074068, 52102159 and 22103013), and Natural Science Foundation of Fujian Province (2022J05091, 2020J02017, 2021J06021, 2021J01190 and 2020J01931).

Declaration of competing interest

The authors have no competing interests to declare that are relevant to the content of this article.

Electronic Supplementary Material

Supplementary material is available in the online version of this article.

References

[1] Yue XM, Xu J, Lin H, *et al*. Beta-SiAlON:Eu^{2+} phosphor-in-glass film: an efficient laser-driven color converter for high-brightness wide-color-gamut projection displays. *Laser Photonics Rev* 2021, **15**: 2100317.

[2] Liao SL, Yang ZZ, Lin JD,*et al*. A hierarchical structure perovskite quantum dots film for laser-driven projection display. *Adv Funct Mater* 2023, **33**: 2210558.

[3] Yang ZZ, Zheng S, Pang T, *et al.* YAG:Ce PiGF@alumina-substrate in a reflection mode for high-brightness laser-driven projection display. *Adv. Mater. Technol* 2023, **8**: 2300132.

[4] Lin SS, Lin H, Chen GX, *et al*. Stable $CsPbBr_3$-glass nanocomposite for low-etendue wide-color-gamut laser-driven projection display. *Laser Photonics Rev* 2021, **15**: 2100044.

[5] Pimputkar S, Speck JS, DenBaars SP, *et al*. Prospects for LED lighting. *Nat Photonics* 2009, **3**: 179-181.

[6] Pust P, Schmidt PJ, Schnick W. A revolution in lighting. *Nat Mater* 2015, **14**: 454-458.

[7] Cho J, Park JH, Kim JK, *et al.* White light-emitting diodes: History, progress, and future. *Laser Photonics Rev* 2017, **11**: 1600147.

[8] Cho J, Schubert EF, Kim JK. Efficiency droop in light-emitting diodes: Challenges and countermeasures. *Laser Photonics Rev* 2013, **7**: 408-421.

[9] Li SX, Wang L, Hirosaki N, *et al*. Color conversion materials for high-brightness laser-driven solid-state lighting. *Laser Photonics Rev* 2018, **12**: 1800173.

[10] Neumann A, Wierer JJ, Davis W, *et. al.* Four-color laser white illuminant demonstrating high color-rendering quality. *Opt Express* 2011, **19**: 982-990.

[11] Kumar V, Dubey AK, Gupta M, *et al*. Speckle noise reduction strategies in laser-based projection imaging, fluorescence microscopy, and digital holography with uniform illumination, improved image sharpness, and resolution. *Opt Laser Technol* 2021, **141**: 107079.

[12] Briers D, Duncan DD, Hirst E, *et al*. Laser speckle contrast imaging: theoretical and practical limitations. *J Biomed Opt* 2013, **18**: 066018.

[13] Yu JB, Si SC, Liu Y, *et al*. High-power laser-driven phosphor-in-glass for excellently high conversion efficiency white light generation for special illumination or display backlighting. *J Mater Chem C* 2018, **6**: 8212-8218.

[14] Wang L, Xie RJ, Suehiro T, *et al*, Down-conversion nitride materials for solid state lighting: Recent advances and perspectives. *Chem Rev* 2018, **118**: 1951-2009.

[15] Zhang YQ, Liu JM, Zhang YJ, *et al*. Robust YAG:Ce single crystal for ultra-high efficiency laser lighting. *J Rare Earths* 2022, **40**: 717-724.

[16] Cantore M, Pfaff N, Farrell RM, *et al*.High luminous flux from single crystal phosphor-converted laser-based white lighting system. *Opt Express* 2016, **24**: A215-A221.

[17] Chen W, Cao DH, Dong YJ, *et al*. Enhancing luminous flux and color rendering of laser-excited YAG:Ce^{3+}single crystal phosphor plate via surface roughening and low-temperature. *J Lumin* 2022, **251**: 119225.

[18] Jiang HJ, Chen LY, Zheng GJ, *et al*. Ultra-Efficient GAGG:Cr^{3+} Ceramic Phosphor-Converted Laser Diode: A promising high-power compact near-infrared light source enabling clear imaging. *Adv Opt Mater* 2022, **10**: 2102741.

[19] Yao Q, Hu P, Sun P, *et.al*. YAG:Ce^{3+} Transparent ceramic phosphors brighten the next-generation laser-driven lighting. *Adv Mater* 2020, **32**: 1907888.

[20] Yang ZY, de Boer T, Braun PM, *et al.* Thermally stable red-emitting oxide ceramics for laser lighting. *Adv Mater* 2023, DOI:10.1002/adma.202301837.

[21] Peng XL, Li SX, Zhang BH, *et al*. Orange-emitting MgO-(Sr,Ba)(3)SiO5:Eu composite phosphor ceramics for turn signals and warm white laser lighting. *J Am Ceram Soc* 2022, **106**: 1945-1953.

[22] Cheng ZQ, Wang YB, Li WY, *et al*. Porous Ce:YAG ceramics with controllable microstructure for high-brightness laser lighting. *J Am Ceram Soc* 2023, **106**: 2903-2910.

[23] Peng Y, Yu ZK, Zhao JZ, *et al*. Unique sandwich design of high-efficiency heat-conducting phosphor-in-glass film for high-quality laser-driven white lighting. *J Adv Ceram* 2022, **11**: 1889-1900.

[24] Wen QX, Wang Y, Zhao C, *et al*. Ultrahigh power density LuAG:Ce green converters for high-luminance laser-driven solid state lighting. *Laser Photonics Rev* 2023, **17**: 2200909.

[25] Lin SS, Lin H, Huang QM, *et al*. Highly crystalline $Y_3Al_5O_{12}$:Ce^{3+} phosphor-in-glass film: a new composite color converter for next-generation high-brightness laser-driven lightings. *Laser Photonics Rev* 2022, **16**: 2200523.

[26] Bao SY, Liang YY, Wang LS, *et al*. Superhigh-luminance Ce:YAG phosphor in glass and

phosphor-in-glass film for laser lighting. *ACS Sustain Chem Eng* 2022, **10**: 8105-8114.

[27] Huang,QG, Sui P, Huang F, *et al*. Toward high-quality laser-driven lightings: chromaticity-tunable phosphor-in-glass film with "phosphor pattern" design. *Laser Photonics Rev* 2022, **16**: 2200040.

[28] Deng TL, Huang LH, Li SX, *et al*. Thermally robust orange-red-emitting color converters for laser-driven warm white light with high overall optical properties. *Laser Photonics Rev* 2022, **16**: 2100722.

[29] Xu J, Yang Y, Wang J, *et al*. Industry-friendly synthesis and high saturation threshold of a LuAG:Ce/glass composite film realizing high-brightness laser lighting. *J Euro Ceram Soc* 2020, **40**: 6031-6036.

[30] Xu YR, Li SX, Zheng P, *et al*. A search for extra-high brightness laser-driven color converters by investigating thermally-induced luminance saturation. *J Mater Chem C* 2019, **7**: 11449-11456.

[31] Xu J, Liu BG, Liu ZW, *et al*. Design of laser-driven SiO_2-YAG:Ce composite thick film: Facile synthesis, robust thermal performance, and application in solid-state laser lighting. *Opt Mater* 2018, **75**: 508-512.

[32] Zhang D, Xiao WG, Liu C,. *et al*. Highly efficient phosphor-glass composites by pressureless sintering. *Nat Commun* 2020, **11**: 2805.

[33] Xiang R, Liang XJ, Li PZ, *et.al*. A thermally stable warm WLED obtained by screen-printing a red phosphor layer on the LuAG:Ce^{3+} PiG substrate. *Chem Eng J* 2016, **306**: 858-865.

[34] Peng Y, Zhao JZ, Yu ZK, *et.al*. High-performance phosphor-in-glass film on thermoelectric generator for non-radiative energy recycling in laser lighting. *Adv Mater Technol* 2023, **8**: 2202162.

[35] Yu ZK, Zhao JZ, Liu JX,. *et.al* Heat-conducting LSN:Ce-in-glass film on AlN substrate for high-brightness laser-driven white lighting. *Ceram Int* 2022, **48**: 36531-36538.

[36] Lin SS, Lin H, Wang PF, *et al*. An orange-yellow-emitting Lu_2-xMg_2Al_2-y$GaySi_2O_{12}$:xCe^{3+} phosphor-in-glass film for laser-driven white light. *J Mater Chem C* 2023, **11**: 1530-1540.

[37] Chen DQ, Xiang WD, Liang XJ, *et al*. Advances in transparent glass-ceramic phosphors for white light-emitting diodes-A review. *J Euro Ceram Soc* 2015, **35**: 859-869.

[38] Berends AC, van de Haar MA, Krames MR, *et al*. YAG:Ce^{3+} Phosphor: from micron-sized workhorse for general lighting to a bright future on the nanoscale. *Chem Rev* 2020, **120**: 13461-

13479.

[39] Liu ZH, Hu P, Jiang HJ, *et al*. $CaAlSiN_3:Eu^{2+}/Lu_3Al_5O_{12}:Ce^{3+}$ phosphor-in-glass film with high luminous efficiency and CRI for laser diode lighting. *J Mater Chem C* 2021, **9**: 3522-3530.

[40] Huang QG, Lin H, Wang B, *et al*. Patterned glass ceramic design for high-brightness high-color-quality laser-driven lightings. *J Adv Ceram* 2022, **11**: 862-873.

[41] Wang LH, Liu JW, Xu L, *et al*. Realizing high-power laser lighting: Artfully importing micrometer BN into Ce: GdYAG phosphor-in-glass film. *Laser Photonics Rev* 2022, **17**: 2200585.

[42] Mou Y, Zhao JZ, Yu ZK, et al. Highly reflective interface design for phosphor-in-glass converter enabling ultrahigh efficiency laser-driven white lighting. *J Eur Ceram Soc* 2022, **42**: 7579-7586.